molbank

MDPI

Communication

Synthesis and Characterization of Hydrazine Bridge Cyclotriphosphazene Derivatives with Amide–Schiff Base Linkages Attached to Decyl and Hydroxy Terminal Groups

Fatin Junaidah Mohamad Fazli and Zuhair Jamain *

Organic Synthesis and Advanced Materials (OSAM) Research Group, Faculty of Science and Natural Resources, Universiti Malaysia Sabah, Jalan UMS, Kota Kinabalu 88400, Malaysia
* Correspondence: zuhairjamain@ums.edu.my

Abstract: New cyclotriphosphazene derivatives featuring amide–Schiff base linkages with a hydrazine bridge and different terminal ends, such as decyl alkyl chains and hydroxy groups, were successfully synthesized and characterized. Fourier-transform infrared spectroscopy (FTIR), nuclear magnetic resonance spectroscopy (NMR), and CHN elemental analysis were used to characterize the structures of these compounds. The formation of hydrazine-bridged cyclotriphosphazene derivatives with amide–Schiff base linkages was confirmed by the FTIR spectra, showing a primary amine band for the amide linkage around ~3300 cm^{-1} and a band for the Schiff base linkage near ~1595 cm^{-1}. This was further supported by NMR analysis, which displayed an amide proton (H-N-C=O) at ~δ 10.00 ppm and an azomethine proton (H-C=N) within the δ 8.40–8.70 ppm range. The ^{31}P NMR spectra of cyclotriphosphazene compounds display a singlet at ~δ 8.20 ppm, indicating an upfield shift that suggests the complete substitution of all phosphorus atoms with identical side chains. Furthermore, CHN analysis verified the purity of the synthesized compounds, with a percentage error below 2%. The introduction of hydrazine bridges and amide–Schiff base linkages into the cyclotriphosphazene core significantly enriches the molecular structure with diverse functional groups. These modifications not only improve the compound's stability and reactivity, but also expand its potential for a wide range of applications.

Keywords: cyclotriphosphazene; amide; Schiff base; hydrazine bridge

check for updates

Citation: Mohamad Fazli, F.J.; Jamain, Z. Synthesis and Characterization of Hydrazine Bridge Cyclotriphosphazene Derivatives with Amide–Schiff Base Linkages Attached to Decyl and Hydroxy Terminal Groups. *Molbank* **2024**, *2024*, M1934. https://doi.org/10.3390/M1934

Academic Editor: R. Alan Aitken

Received: 1 November 2024
Revised: 1 December 2024
Accepted: 5 December 2024
Published: 7 December 2024

Copyright: © 2024 by the authors. Licensee MDPI, Basel, Switzerland. This article is an open access article distributed under the terms and conditions of the Creative Commons Attribution (CC BY) license (https://creativecommons.org/licenses/by/4.0/).

1. Introduction

The exploration of cyclotriphosphazene derivatives arose from environmental issues since those compounds release toxic and corrosive substances during decomposition [1,2]. Modifying traditional cyclotriphosphazene into derivatives offers significant advantages and broader application potential, not only as flame retardant materials but also as additives in various fields [3–6]. Cyclotriphosphazene derivatives are derived from hexachlorocyclotriphosphazene (HCCP), as shown in Figure 1, which features a classical heterocyclic ring structure with alternating phosphorus and nitrogen atoms, along with two chlorine substituents on the phosphorus atoms that can be easily replaced by various nucleophiles [7,8].

The variation of nucleophiles leads to changes in the chemical and physical properties of each cyclotriphosphazene compound, resulting in additional beneficial characteristics [9]. Cyclotriphosphazenes are typically effective as flame retardants because their structure contains two active elements, phosphorus and nitrogen, which are known for their strong flame-retardant qualities [10]. The development of cyclotriphosphazene derivatives with unique functional properties relies on the number of substituents, as well as the regiochemistry and stereochemistry involved in the reactions between HCCP and nucleophiles. Recent investigations have increasingly focused on cyclotriphosphazene derivatives due to their wide-ranging contributions and valuable properties [11,12].

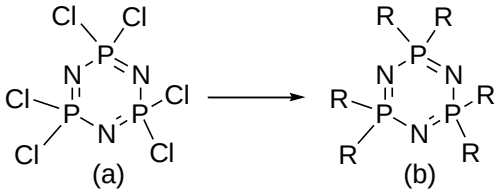

Figure 1. (**a**) The structure of hexachlorocyclotriphosphazene and (**b**) cyclotriphosphazene after being introduced to any side group.

Previous studies have been conducted by modifying the -R side group of phosphazene, such as -NH_2, -OR, -OC_6H_5 or fluorinated derivatives, which can improve oxidative and thermal stabilities [13]. Furthermore, the properties of polyphosphazenes depend significantly on the materials to which they are applied, adjusting and controlling the various side groups that influence elasticity, electro-optical properties, biological utility, solvent resistance, and thermal stability [14–17]. A wide range of polyphosphazenes, synthesized with diverse side groups, provides a valuable platform for studying the structure–property relationships within polyphosphazene systems. The characteristics of these polymers are influenced by two main factors: the unique structure of the backbone and the structure of the phosphorus-linked side groups [18].

Polyphosphazenes have unique characteristics because of their inorganic backbone, but the P–N bonds are still not fully understood. The inorganic backbone has a low barrier to torsion, with a low energy barrier of 0.1 to 0.5 Kcal per repeating unit, giving polyphosphazenes high flexibility even at temperatures as low as 100 °C, where they undergo a glass transition [19]. Allcock explains that the polymer chains have a wide range of molecular mobility due to the symmetrical cylinder of the P–N bond, which overlaps the nitrogen *p*-orbital with any of the five phosphorous *d*-orbitals. Unlike other macromolecular or unsaturated structures, there is no conjugation or delocalization of π-electrons in P–N, regardless of its backbone chain configuration that alternates double and single bonds [20–22].

Polyphosphazene polymers are naturally fire-resistant because of the phosphorus in their inorganic backbone [23]. Phosphorous-based compounds are used in a variety of flame-retardant applications because phosphorous can boost char in the condensed phase while inhibiting flame in the gas phase. X-rays and γ-rays do not cause the backbone to separate. The peculiar traits can be linked to the polar P–N's unwillingness to break into free radicals when exposed to heat or radiation. Furthermore, the backbone contributes to the higher base refractive index here than in most other polymers, which is of importance in the electro-optical sector [24]. The characteristics of polyphosphazene polymers depend on the side groups attached to phosphorous. Chemical characteristics, solubility and solid-state properties are some of the traits that side groups can regulate [25].

Hence, new hydrazine-bridged cyclotriphosphazene derivatives with amide–Schiff base linkages were synthesized to investigate the chemical structures of these compounds. The incorporation of hydrazine bridges and the presence of amide–Schiff base linkages introduce multiple functional groups into the cyclotriphosphazene core, which contribute to the compound's stability, reactivity, and potential applications. The amide linkage provides hydrogen bonding sites that can increase thermal stability, while the Schiff base linkage, with its azomethine group (C=N), contributes to the rigidity and electron-donating properties. Furthermore, these features make the compounds interesting for studying interactions they could enhance fire-retardant behavior and other potential uses in material science.

2. Results and Discussion

2.1. Synthesis Flow

The alkylation of methyl-4-hydroxybenzoate with 1-bromodecane, followed by a saponification process, produced intermediate **1a** (Scheme 1) [26]. Intermediates **2a–b** were prepared by the reaction of the acid chloride of the 4-substituted benzoic acid with 4-aminobenzaldehyde, and were subsequently used to produce intermediates **3a–b** (Scheme 2) [27]. The reaction of phosphonitrilic chloride trimer with 4-hydroxybenzaldehyde yielded compound **4** (Scheme 3) [28], which was further reacted to form the final compounds **5a–b** (Scheme 4) [29–31].

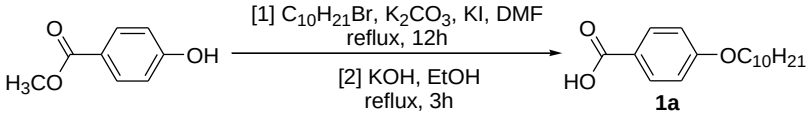

Scheme 1. Alkylation reaction of intermediate **1a**.

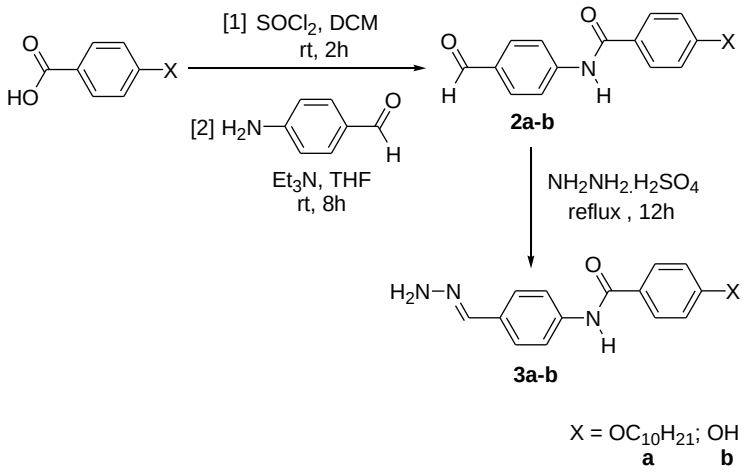

Scheme 2. Formation of intermediates **2a–b** and **3a–b**.

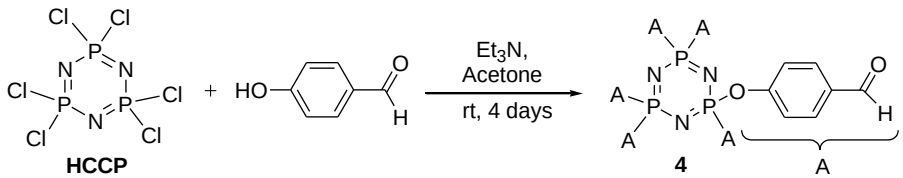

Scheme 3. Formation of hexasubstituted cyclotriphosphazene intermediate **4**.

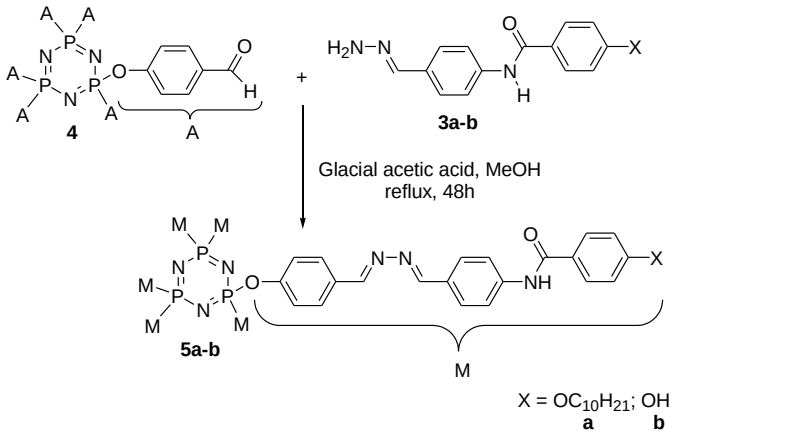

Scheme 4. Formation of hexasubstituted cyclotriphosphazene compounds **5a–b**.

2.2. FTIR Spectral Discussion

The structures of all intermediates and final compounds were analyzed with FTIR to identify the functional groups present in the compounds. The FTIR data for intermediate **1a**, which contains a decyl chain, show an O–H stretching absorption band at 3342.35 cm^{-1}. The symmetrical and asymmetrical $C_{sp}{}^3$-H stretching vibrations are observed at 2920.13 and 2851.34 cm^{-1}, respectively. The C=O stretching appears at 1717.48 cm^{-1}, followed by the C=C aromatic stretching at 1597.55 cm^{-1}. Besides this, the C-O stretching is indicated at 1250.52 cm^{-1}. The presence of the O-H stretching band confirms the success of the alkylation reaction through the deprotonation of the methoxy group.

The FTIR data of intermediate **2a** show the appearance of absorption bands of N–H stretching at 3312.76 cm^{-1} and C=O stretching at 1634.83 cm^{-1}, indicating the successful formation of an amide linkage. The other band at 1567.35 cm^{-1} was assigned to C=C stretching, and C–O stretching can be seen at 1158.98 cm^{-1}. The structural differences of intermediates **2a** and **2b** can be distinguished by the presence of $C_{sp}{}^3$-H stretching at 2913.16 and 2804.96 cm^{-1} in **2a** for decyl terminal chains, while the O-H stretching at 3662.64 cm^{-1} in **2b** indicates a hydroxyl group attached at the terminal end.

The IR spectrum data for intermediate **3a** show several absorption bands corresponding to its basic structure, including N–H stretching at 3320.94 cm^{-1}, C=O stretching at 1680.18 cm^{-1}, and C=N stretching at 1596.16 cm^{-1}. Moreover, C=C stretching appears at 1514.54 cm^{-1}, followed by C–N stretching at 1127.07 cm^{-1}. Each structure can be distinguished by the different absorption bands, with the alkyl group in **3a** exhibiting $C_{sp}{}^3$-H stretching at 2917.62 and 2869.38 cm^{-1}, while the hydroxy group (**3b**) shows O–H stretching at 3467.71 cm^{-1}. The FTIR spectrum of intermediate **4** displays absorption bands at 1702.89, 1584.67, and 1205.03 cm^{-1} for C=O, C=C, and C-O stretching, respectively. The presence of the cyclotriphosphazene core is confirmed by the P=N stretching at 1152.79 cm^{-1} and P–O–C bending at 959.44 cm^{-1}.

Based on the overlay FTIR spectra of compounds **5a–b** (Figure 2), the presence of Schiff base–amide with a hydrazine bridge linkage confirms the success of this reaction. The existence of C=N stretching at 1595.64 cm^{-1} for **5a**, and 1595.41 cm^{-1} for **5b**, indicates the successful formation of the Schiff base linkage. The absorption band at 1530.01 cm^{-1} corresponds to C=C stretching in the aromatic benzene ring, while the peak at 1298.02 cm^{-1} is attributed to C–O stretching. The existence of cyclotriphosphazene in each structure is confirmed by the P=N vibration at 1151.82 cm^{-1} and P–O–C bending at 951.83 cm^{-1}. Meanwhile, the presence of $C_{sp}{}^3$-H stretching at 2932.53 and 2857.62 cm^{-1} in compound **5a** denotes decyl chains, while the O–H stretching at 3364.53 cm^{-1} can be seen in compound **5b**.

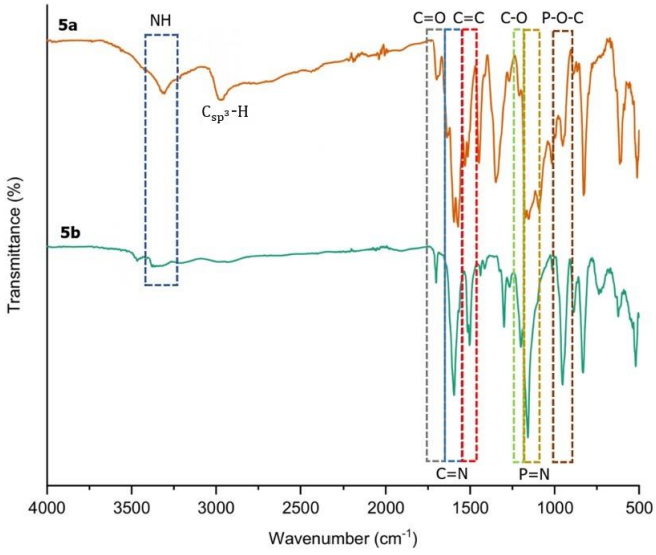

Figure 2. The overlay FTIR spectra of compounds **5a** and **5b**.

2.3. NMR Spectral Discussion

Compound **5b** was chosen as a representative example to confirm the assigned chemical shifts of the molecules. Figure 3 depicts the structure of compound **5b** with detailed atomic numbering, while Figure 4 presents the ^{1}H NMR spectrum of compound **5b**.

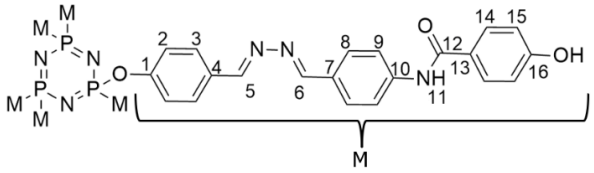

Figure 3. Chemical structure of compound **5b** with complete atomic numbering.

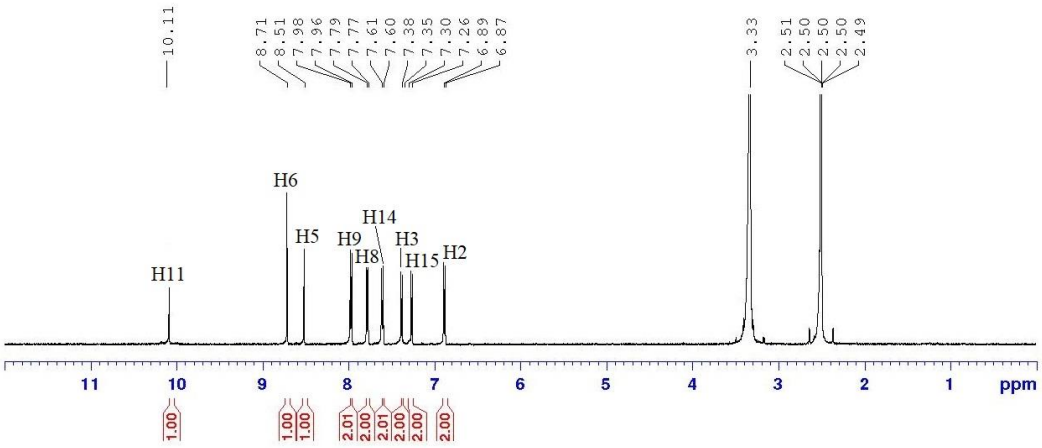

Figure 4. ^{1}H NMR (500 MHz, DMSO-d_6) spectrum of compound **5b**.

The structure of compound **5b**, as revealed by its ^{1}H NMR spectrum (Figure 4), shows a singlet signal at the downfield region of δ 10.11 ppm (H11), which corresponds to the proton of the amide group. In addition, the signals at δ 8.71 (H6) and δ 8.51 ppm (H5) appear as two singlets, indicating the presence of two protons from the azomethine linkages. In the aromatic region, signals at δ 7.97, 7.78, 7.61, 7.37, 7.28, and 6.88 ppm are observed as doublets, representing 12 aromatic protons from three benzene rings in the structure. These signals are assigned to protons H9, H8, H14, H3, H15, and H2, respectively. H9 and H8 protons experience more downfield shift than other aromatic protons, attributed to the high polarizability of the surrounding electronic environment [32]. This increased polarizability enhances the electron-withdrawing effects, thereby deshielding H9 and H8. As a result, these protons shift further downfield in the NMR spectrum, reflecting the influence of nearby polarizable groups or atoms that reduce electron density around them.

The ^{13}C NMR spectrum of compound **5b** (Figure 5) reveals the presence of 15 carbon signals, each corresponding to different structural features within the molecule. Among these, two signals are attributed to the carbons of the azomethine groups, C6 and C5, which resonate at δ 157.70 and 155.10 ppm, respectively. Meanwhile, one signal at the most downfield region corresponds to the carbon in the amide functional group (C12), which appears at δ 166.30 ppm. Six signals represent the aromatic carbons resonating at δ 131.11, 129.51, 124.36, 124.09, 123.57, and 116.30, which were assigned to C9, C8, C14, C3, C15, and C2, respectively. Moreover, six more signals corresponding to quaternary carbons were assigned at δ 161.51 (C1), 150.40 (C16), 148.78 (C10), 142.55 (C7), 142.09 (C4), and 136.98 (C13), corresponding to carbons that are not directly bonded to any hydrogen atoms. The presence of electronegative functional groups significantly influences the chemical shifts observed in the ^{13}C NMR spectrum. These functional groups withdraw electron density from nearby carbon atoms, causing deshielding effects that shift the carbon signals

downfield to higher δ values [33]. This shift variation allows the NMR spectrum to provide insights into the electronic environment and the proximity of carbons to electronegative substituents or linkages [34,35].

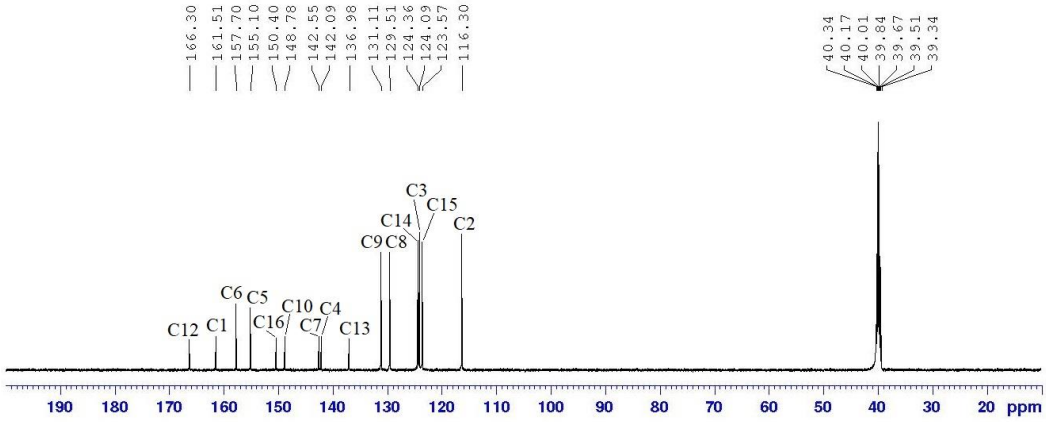

Figure 5. ^{13}C NMR (125 MHz, DMSO-d$_6$) spectrum of compound **5b**.

The ^{31}P NMR spectrum of compound **5b** (Figure 6a) shows a singlet at δ 8.24 ppm, shifted upfield compared to HCCP (δ 20.00 ppm), which contains six electron–withdrawing chlorine atoms (Figure 6b). This upfield shift suggests that all phosphorus atoms are fully substituted with identical side chains. The presence of six side chains with high electron density enhances the shielding effect, contributing to the observed chemical shift [36].

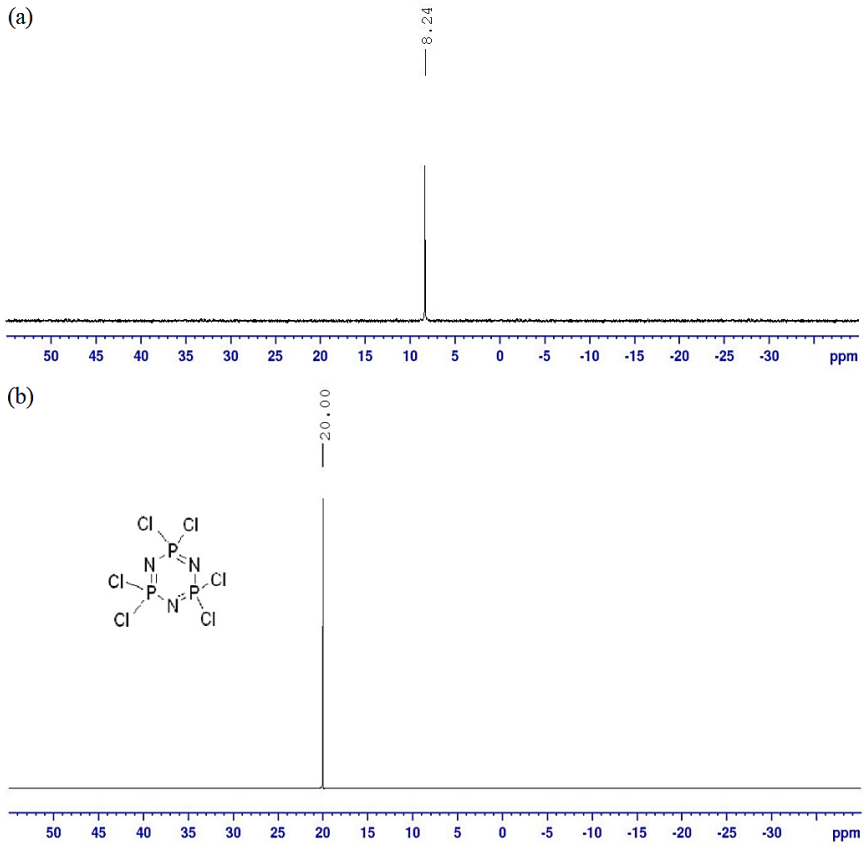

Figure 6. ^{31}P NMR spectra (500 MHz, DMSO-d$_6$) of (**a**) compound **5b** and (**b**) HCCP.

2.4. CHN Elemental Analysis

The percentages of carbon (C), hydrogen (H), and nitrogen (N) in the compounds are summarized in Table 1. These values demonstrate the purity of the compounds, as the percentage errors for each element were less than 2%. Such minimal errors indicate a high level of purity, with the actual elemental composition closely matching the theoretical values expected for the compounds' structures. This low deviation confirms the accuracy of the synthesis process.

Table 1. The percentages of carbon, hydrogen and nitrogen in the intermediate and final compounds.

Compound	% Found (*Calculated*)		
	C (%)	**H (%)**	**N (%)**
1a	73.29 (*73.34*)	9.34 (*9.41*)	-
2a	75.50 (*75.56*)	8.14 (*8.19*)	3.62 (*3.67*)
2b	69.62 (*69.70*)	4.53 (*4.60*)	5.77 (*5.81*)
3a	72.81 (*72.88*)	8.36 (*8.41*)	10.57 (*10.62*)
3b	65.83 (*65.87*)	5.10 (*5.13*)	16.41 (*16.46*)
4	58.47 (*58.55*)	3.49 (*3.51*)	4.84 (*4.88*)
5a	71.40 (*71.45*)	6.93 (*6.96*)	9.37 (*9.41*)
5b	66.18 (*66.22*)	4.20 (*4.23*)	12.84 (*12.87*)

3. Materials and Methods

3.1. Chemicals

In this study, the chemicals and solvents used are 1-bromodecane, 4-hydroxybenzoic acid, methyl-4-hydroxybenzoate, 4-hydroxybenzaldehyde, 4-aminobenzaldehyde, phosphonitrilic chloride trimer, potassium iodide, potassium carbonate, dimethylformamide, dichloromethane, triethylamine, hydrazinium sulphate, methanol, ethanol, acetone and glacial acetic acid. All these solvent and chemicals were purchased and used without purification from Sigma-Aldrich (Steinheim, Germany), Merck (Darmstadt, Germany), Acros Organics (Geel, Belgium), BDH laboratory (British Drug Houses) (Nichiryo, Japan), and QREC (Asia) (Selangor, Malaysia).

3.2. Instrumentation

All the synthesized compounds were characterized using Fourier Transform Infrared spectroscopy (FTIR) of Bruker ALPHA II in order to identify their functional groups. This was performed through attenuated total reflectance (ATR) between 500 and 4000 cm^{-1}. Nuclear magnetic resonance (NMR) spectroscopy was used to determine the molecular structure of the compounds by analyzing the ^{1}H, ^{13}C, and ^{31}P nuclei. The analysis was obtained by a Bruker 500 MHz Ultrashield spectrometer using $CDCl_3$ and DMSO-d_6 as a solvent system. About 20 mg of sample was dissolved in a deuterated solvent before being transferred into an NMR tube. The FTIR and NMR spectra of all the intermediates and compounds are summarized in the Supplementary Materials, Figures S1–S24. CHN elemental analysis was used to determine the purity of all the synthesized compounds by measuring the percentages of carbon (C), hydrogen (H), and nitrogen (N), and comparing the experimental results with theoretical values.

3.3. Synthesis Method

3.3.1. Synthesis of 4-(Decyloxy)benzoic Acid, **1a**

Here, 0.08 mol of methyl-4-hydroxybenzoate and 0.08 mol of 1-bromohexane were dissolved in 40 mL of dimethylformamide (DMF) separately. Both solutions were mixed in a 250 mL round bottom flask; 0.13 mol of potassium carbonate (K_2CO_3) and 0.008 mol of potassium iodide (KI) were added to the mixture, which then refluxed for 12 h. The reaction progress was monitored using a thin-layer chromatograph (TLC). The mixture was poured into 500 mL of cold water upon completion, filtered, and dried in vacuum overnight. The precipitate was then mixed with 0.13 mol of potassium hydroxide in 50 mL of ethanol and refluxed for 3 h. Upon completion, the mixture was poured into cold water, filtered, and dried in a vacuum overnight.

Yield = 29.55 g (97.18%), white powder. FTIR (cm^{-1}): 3342.35 (O-H stretching), 2920.13 and 2851.34 (Csp^3-H stretching), 1717.48 (C=O stretching), 1597.55 (C=C stretching), 1250.52 (C-O stretching). ^{1}H-NMR (500 MHz, DMSO-d_6) δ, ppm: 11.00 (s, 1H), 7.78 (d, J = 6 Hz, 2H), 6.73 (d, J = 6 Hz, 2H), 3.96 (t, J = 9 Hz, 2H), 1.68–1.73 (m, 2H), 1.40–1.46 (m, 2H), 1.29–1.36 (m, 12H), 0.87 (t, J = 6 Hz, 3H). ^{13}C-NMR (125 MHz, DMSO-d_6) δ, ppm: 168.78, 159.00, 134.78, 130.36, 112.83, 67.73, 31.13, 28.82, 28.79, 28.77, 28.62, 28.47, 25.45, 21.85, 13.60. CHN elemental analysis calculated for $C_{17}H_{26}O_3$: C: 73.34%, H: 9.41%; Found: C: 73.29%, H: 9.34%.

3.3.2. Synthesis of 4-{[4-(Substituted)benzoyl]amino}benzoic Acid, **2a–b**

Here, 6 mL of thionyl chloride and 40 mL of dichloromethane were added to 0.05 mol of intermediate **1a** in 150 mL round bottom flask, then left for 2 h at room temperature. A solution of 0.05 mol 4-aminobenzaldehyde in 20 mL of THF was added dropwise to the mixture; 2 mL of triethylamine was added and the mixture was left with stirring for 8 h at room temperature. The reaction's progress was monitored by TLC. The precipitate was filtered and dried. The dried precipitate was recrystallized with methanol. The same method was used to synthesize intermediate **2b**.

4-{[4-(Decyloxy)benzoyl]amino}benzoic Acid, **2a**

Yield = 4.90 g (76.20%), black powder. FTIR (cm^{-1}): 3312.76 (N-H stretching), 2913.16 and 2804.96 (Csp^3-H stretching), 1634.83 (C=O stretching), 1567.35 (C=C stretching), 1158.98 (C-O stretching). ^{1}H-NMR (500 MHz, DMSO-d_6) δ, ppm: 10.33 (s, 1H), 9.70 (s, 1H), 8.19 (d, J = 6 Hz, 2H), 7.99 (d, J = 6 Hz, 2H), 7.95 (d, J = 6 Hz, 2H), 7.03 (d, J = 6 Hz, 2H), 4.07 (t, J = 9 Hz, 2H), 1.70–1.76 (m, 2H), 1.39–1.45 (m, 2H), 1.26–1.34 (m, 12H), 0.85 (t, J = 6 Hz, 3H). ^{13}C-NMR (125 MHz, DMSO-d_6) δ, ppm: 190.01, 166.18, 162.51, 146.05, 143.24, 130.29, 126.72, 124.89, 120.51, 114.93, 68.66, 31.59, 29.24, 29.20, 29.02, 28.99, 28.92, 25.80, 22.32, 14.06. CHN elemental analysis that calculated for $C_{24}H_{31}NO_3$: C: 75.56%, H: 8.19%, N: 3.67%; Found: C: 75.50%, H: 8.14%, N: 3.62%.

4-{[4-(Hydroxy)benzoyl]amino}benzoic Acid, **2b**

Yield = 11.57 g (89.33%), black powder. FTIR (cm^{-1}): 3662.64 (O-H stretching), 3343.92 (N-H stretching), 1675.20 (C=O stretching), 1574.67 (C=C stretching). ^{1}H-NMR (500 MHz, DMSO-d_6) δ, ppm: 10.07 (s, 1H), 9.62 (s, 1H), 8.09 (m, 4H), 7.98 (d, J = 6 Hz, 2H), 6.90 (d, J = 6 Hz, 2H). ^{13}C-NMR (125 MHz, DMSO-d_6) δ, ppm: 190.55, 167.03, 164.32, 140.06, 139.29, 136.08, 130.55, 129.94, 126.57, 116.19. CHN elemental analysis that calculated for $C_{14}H_{11}NO_3$: C: 69.70%, H: 4.60%, N: 5.81%; Found: C: 69.62%, H: 4.53%, N: 5.77%.

3.3.3. Synthesis of 4-[4-(Substituted-Hydrazonomethyl)phenyl]benzamide, **3a–b**

Here, 0.03 mol of hydrazine sulfate was dissolved in 75 mL of hot distilled water; 0.10 mol of sodium acetate anhydrous was added to the solution with stirring. The mixture was left to boil for 5 min and we let the temperature cool down to 50 °C before 75 mL of hot ethanol was added and stirred until a cloudy solution formed. The precipitate was removed by filtration and the filtrate was poured into a 250 mL round bottom flask that contained

0.03 mol of intermediate **2a**. The mixture was stirred for 12 h at room temperature. The precipitate was filtered upon completion and dried. The dried precipitate was recrystallized using acetone. This method was repeated to synthesize **3b**.

4-[4-(Decyloxy-Hydrazonomethyl)phenyl]benzamide, **3a**

Yield = 1.21 g (79.29%), dark orange powder. FTIR (cm^{-1}): 3320.94 (N-H stretching), 2917.62 and 2869.38 (Csp^3-H stretching), 1680.18 (C=O stretching), 1596.16 (C=N stretching), 1514.54 (C=C stretching), 1256.59 (C-O stretching), 1127.07 (C-N stretching). ^{1}H-NMR (500 MHz, DMSO-d_6) δ, ppm: 10.01 (s, 1H), 8.47 (s, 1H), 7.79 (d, J = 6 Hz, 2H), 7.05 (d, J = 6 Hz, 2H), 7.00 (d, J = 6 Hz, 2H), 6.64 (d, J = 6 Hz, 2H), 5.02 (d, J = 6 Hz, 2H), 4.05 (d, J = 6 Hz, 2H), 1.77 (d, J = 6 Hz, 2H), 1.73 (d, J = 6 Hz, 2H), 1.30–1.46 (m, 12H), 0.88 (t, J = 6 Hz, 3H). ^{13}C-NMR (125 MHz, DMSO-d_6) δ, ppm: 165.01, 161.32, 154.61, 147.55, 141.37, 139.43, 130.02, 122.36, 115.38, 115.06, 68.58, 31.64, 29.31, 29.27, 29.16, 29.10, 28.98, 25.90, 22.35, 14.07. CHN elemental analysis that calculated for $C_{24}H_{33}N_3O_2$: C: 72.88%, H: 8.41%, N: 10.62%; Found: C: 72.81%, H: 8.36%, N: 10.57%.

4-[4-(Hydroxy-Hydrazonomethyl)phenyl]benzamide, **3b**

Yield = 2.22 g (92.08%), dark brown powder. FTIR (cm^{-1}): 3467.71 (O-H stretching), 3310.54 (N-H stretching), 1685.84 (C=O stretching), 1592.76 (C=N stretching), 1513.77 (C=C stretching), 1297.57 (C-O stretching), 1165.80 (C-N stretching). ^{1}H-NMR (500 MHz, DMSO-d_6) δ, ppm: 10.00 (s, 1H), 8.42 (s, 1H), 7.69 (d, J = 6 Hz, 2H), 7.04 (d, J = 6 Hz, 2H), 6.84 (d, J = 6 Hz, 2H), 6.58 (d, J = 6 Hz, 2H), 5.08 (d, J = 6 Hz, 2H). ^{13}C-NMR (125 MHz, DMSO-d_6) δ, ppm: 164.78, 160.55, 157.38, 156.11, 143.68, 130.63, 128.37, 122.59, 116.11, 116.03. CHN elemental analysis that calculated for $C_{14}H_{13}N_3O_2$: C: 65.87%, H: 5.13%, N: 16.46%; Found: C: 65.83%, H: 5.10%, N: 16.41%.

3.3.4. Synthesis of Hexakis(4-Formlyphenoxy)cyclotriphosphazene, **4**

Here, 0.08 mol of 4-hydroxybenzaldehyde and 0.1 mol of triethylamine were dissolved in 150 mL of acetone, and the mixture was cooled to 0 °C in an ice bath. The mixture was stirred for 30 min, while 0.01 mol of phosphonitrilic chloride trimer was dissolved in 50 mL of acetone and then added dropwise to the mixture. The temperature was maintained within 0 °C for 2 h. Then, the mixture was allowed to attain room temperature with continued stirring for 4 days. The mixture was monitored using TLC. Upon completion, the mixture was poured into 250 mL of cold distilled water, and the resulting precipitate was filtered and dried.

Yield = 11.63 g (87.54%), white powder. FTIR (cm^{-1}): 1702.89 (C=O stretching), 1584.67 (C=C stretching), 1205.03 (C-O stretching), 1152.79 (P=N stretching), 959.44 (P-O-C stretching). ^{1}H-NMR (500 MHz, DMSO-d_6) δ, ppm: 9.90 (s, 1H), 7.78 (d, J = 6 Hz, 2H), 7.16 (d, J = 6 Hz, 2H). ^{13}C-NMR (125 MHz, DMSO-d_6) δ, ppm: 191.69, 153.59, 133.55, 131.46, 121.03. ^{31}P-NMR (500 MHz, DMSO-d_6) δ, ppm: 7.60. CHN elemental analysis that calculated for $C_{42}H_{30}N_3O_{12}P_3$: C: 58.55%, H: 3.51%, N: 4.88%; Found: C: 58.47%, H: 3.49%, N: 4.84%.

3.3.5. Synthesis of Hexakis{4-((E)-((4-((E)-4-Substituted-Benzylidene)hydrazine-1-Ylidene) hydrazonomethyl)phenoxy}triphosphazene, **5a–b**

Here, 1 mmol of intermediate **4** and 8 mmol of intermediate **3a** were mixed in 40 mL of methanol. Five drops of glacial acetic acid were added into the mixture and stirred for 2 days in room temperature. The reaction progress was monitored by TLC. The mixture was cooled in ice water upon completion and the precipitate formed was filtered then dried. The dried precipitate was recrystallized from methanol. This method was repeated to synthesize compound **5b**.

Hexakis{4-((E)-((4-((E)-4-Decyloxy-Benzylidene)hydrazine-1-Ylidene)hydrazonomethyl) phenoxy}triphosphazene, **5a**

Yield = 0.88 g (85.72%), dark red powder. FTIR (cm^{-1}): 3301.40 (N-H stretching), 2932.53 and 2857.62 (Csp^3-H stretching), 1692.78 (C=O stretching), 1595.64 (C=N stretching), 1530.01 (C=C stretching), 1298.02 (C-O stretching), 1151.82 (P=N stretching), 951.83 (P-O-C stretching). ^{1}H-NMR (500 MHz, DMSO-d_6) δ, ppm: 10.03 (s, 1H), 8.66 (s, 1H), 8.55 (s, 1H), 7.96 (d, J = 6 Hz, 2H), 7.87 (d, J = 6 Hz, 2H), 7.56 (d, J = 6 Hz, 2H), 7.33 (d, J = 6 Hz, 2H), 7.28 (d, J = 6 Hz, 2H), 7.04 (d, J = 6 Hz, 2H), 4.07 (t, J = 9 Hz, 2H), 1.73–1.79 (m, 2H), 1.45–1.48 (m, 2H), 1.30–1.44 (m, 12H), 0.88 (t, J = 6 Hz, 3H). ^{13}C-NMR (125 MHz, DMSO-d_6) δ, ppm: 165.03, 162.02, 159.06, 158.48, 150.63, 149.14, 143.56, 136.48, 135.76, 130.75, 130.54, 129.29, 122.33, 122.09, 115.46, 68.63, 31.64, 29.28, 29.15, 29.13, 28.94, 25.90, 22.36, 14.07. ^{31}P-NMR (500 MHz, DMSO-d_6)δ, ppm: 8.20. CHN elemental analysis that calculated for $C_{186}H_{216}N_{21}O_{18}P_3$: C: 71.45%, H: 6.96%, N: 9.41%; Found: C: 71.40%, H: 6.93%, N: 9.37%.

Hexakis{4-((E)-((4-((E)-4-Hydroxy-Benzylidene)hydrazine-1-Ylidene)hydrazonomethyl) phenoxy}triphosphazene, **5b**

Yield = 2.11 g (77.13%), golden yellow powder. FTIR (cm^{-1}): 3364.53 (O-H stretching), 3310.01 (N-H stretching), 1697.92 (C=O stretching), 1595.41 (C=N stretching), 1503.80 (C=C stretching), 1299.21 (C-O stretching), 1158.09 (P=N stretching), 952.69 (P-O-C stretching). ^{1}H-NMR (500 MHz, DMSO-d_6) δ, ppm: 10.11 (s, 1H), 8.71 (s, 1H), 8.51 (s, 1H), 7.97 (d, J = 6 Hz, 2H), 7.78 (d, J = 6 Hz, 2H), 7.61 (d, J = 6 Hz, 2H), 7.37 (d, J = 6 Hz, 2H), 7.28 (d, J = 6 Hz, 2H), 6.88 (d, J = 6 Hz, 2H). ^{13}C-NMR (125 MHz, DMSO-d_6) δ, ppm: 166.30, 161.51, 157.70, 155.10, 150.40, 148.78, 142.55, 142.09, 136.98, 131.11, 129.51, 124.36, 124.09, 123.57, 116.30. ^{31}P-NMR (500 MHz, DMSO-d_6) δ, ppm: 8.24. CHN elemental analysis that calculated for $C_{126}H_{96}N_{21}O_{18}P_3$: C: 66.22%, H: 4.23%, N: 12.87%; Found: C: 66.18%, H: 4.20%, N: 12.84%.

4. Conclusions

The new hexasubstituted cyclotriphosphazene derivatives were successfully synthesized through the formation of amide–Schiff base linkages with hydrazine bridges. These derivatives feature different terminal groups, including a decyl chain (**5a**) and hydroxy group (**5b**). In summary, FTIR spectra confirmed the formation of hydrazine-bridged cyclotriphosphazene derivatives with amide–Schiff base linkages, showing distinctive bands at ~3300 cm^{-1} for the amide linkage and ~1595 cm^{-1} for the Schiff base linkage. NMR analysis supported these findings, with amide protons at ~δ 10.00 ppm and azomethine protons in the δ 8.40–8.70 ppm range. The ^{31}P NMR spectrum revealed a singlet at ~δ 8.20 ppm, indicating complete substitution of all phosphorus atoms with identical side chains. CHN analysis further verified the compounds' high purity, with a percentage error below 2%. The incorporation of hydrazine bridges and amide–Schiff base linkages into the cyclotriphosphazene core improves the compound's stability and reactivity, while also broadening its potential for diverse applications. The hydrazine bridges strengthen the molecular structure, and the amide–Schiff base linkages introduce reactive sites that can facilitate further chemical interactions. This multifunctional design increases the compound's versatility, making it suitable for a range of applications in fields such as coatings, polymers, and composite materials to improve flame resistance and enhance safety.

Supplementary Materials: Figure S1. The FTIR spectrum of intermediate **1a**; Figure S2. The FTIR spectrum of intermediate **2a**; Figure S3. The FTIR spectrum of intermediate **2b**; Figure S4. The FTIR spectrum of intermediate **3a**; Figure S5. The FTIR spectrum of intermediate **3b**; Figure S6. The FTIR spectrum of intermediate **4**; Figure S7. The FTIR spectrum of compound **5a**; Figure S8. The FTIR spectrum of compound **5a**; Figure S9. ^{1}H NMR (500 MHz, DMSO-d_6) spectrum of intermediate **1a**; Figure S10. ^{13}C NMR (125 MHz, DMSO-d_6) spectrum of intermediate **1a**; Figure S11. ^{1}H NMR (500 MHz, DMSO-d_6) spectrum of intermediate **2a**; Figure S12. ^{13}C NMR (125 MHz, DMSO-d_6) spectrum of intermediate **2a**; Figure S13. ^{1}H NMR (500 MHz, DMSO-d_6) spectrum of intermediate **2b**; Figure S14. ^{13}C NMR (125 MHz, DMSO-d_6) spectrum of intermediate **2b**; Figure S15. ^{1}H NMR

(500 MHz, DMSO-d_6) spectrum of intermediate **3a**; Figure S16. ^{13}C NMR (125 MHz, DMSO-d_6) spectrum of intermediate **3a**; Figure S17. ^{1}H NMR (500 MHz, DMSO-d_6) spectrum of intermediate **3b**; Figure S18. ^{13}C NMR (125 MHz, DMSO-d_6) spectrum of intermediate **3b**; Figure S19. ^{1}H NMR (500 MHz, DMSO-d_6) spectrum of intermediate **4**; Figure S20. ^{13}C NMR (125 MHz, DMSO-d_6) spectrum of intermediate **4**; Figure S21. ^{31}P NMR (500 MHz, DMSO-d_6) spectrum of intermediate **4**; Figure S22. ^{1}H NMR (500 MHz, DMSO-d_6) spectrum of compound **5a**; Figure S23. ^{13}C NMR (125 MHz, DMSO-d_6) spectrum of compound **5a**; Figure S24. ^{31}P NMR (500 MHz, DMSO-d_6) spectrum of compound **5a**; Figure S25. ^{1}H NMR (500 MHz, DMSO-d_6) spectrum of compound **5b**; Figure S26. ^{13}C NMR (125 MHz, DMSO-d_6) spectrum of compound **5b**; Figure S27. ^{31}P NMR (500 MHz, DMSO-d_6) spectrum of compound **5b**.

Author Contributions: Conceptualization, Z.J.; methodology, Z.J.; software, Z.J. and F.J.M.F.; validation, Z.J. and F.J.M.F.; formal analysis, Z.J. and F.J.M.F.; investigation, F.J.M.F.; resources, Z.J.; data curation, Z.J. and F.J.M.F.; writing—original draft preparation, Z.J. and F.J.M.F.; writing—review and editing, Z.J. and F.J.M.F.; visualization, Z.J. and F.J.M.F.; supervision, Z.J.; project administration, Z.J.; funding acquisition, Z.J. All authors have read and agreed to the published version of the manuscript.

Funding: This research was funded by Universiti Malaysia Sabah (UMS) with grant number GUG0679-1/2024 and the APC was funded by the correspondence.

Data Availability Statement: The original contributions presented in the study are included in the article/Supplementary Materials. Further inquiries can be directed to the corresponding author.

Acknowledgments: The authors gratefully acknowledged the lab facility support from Universiti Malaysia Sabah (UMS) and Universiti Sains Malaysia (USM).

Conflicts of Interest: The authors declare no conflicts of interest.

References

1. Jeevananthan, V.; Shanmugan, S. Halogen-free layered double hydroxide-cyclotriphosphazene carboxylate flame retardants: Effects of cyclotriphosphazene di, tetra and hexacarboxylate intercalation on layered double hydroxides against the combustible epoxy resin coated on wood substrates. *RSC Adv.* **2022**, *12*, 23322–23336. [CrossRef] [PubMed]
2. Jamain, Z.; Azman, A.N.A.; Razali, N.A.; Makmud, M.Z.H. A Review on Mesophase and Physical Properties of Cyclotriphosphazene Derivatives with Schiff Base Linkage. *Crystals* **2022**, *12*, 1174. [CrossRef]
3. Yang, Y.; Zhang, Q.; Hao, Y.; Lan, X.; Haurie, L.; Zheng, D.; Huang, G. Preparation of a cyclotriphosphazene microsphere bearing a phosphaphenanthrene structure towards fire-safety and mechanical enhancement for epoxy and its aramid fiber composite. *Mater. Adv.* **2024**, *5*, 2860–2871. [CrossRef]
4. Ali, S.; Zuhra, Z.; Butler, I.S.; Dar, S.U.; Hameed, M.U.; Wu, D.; Zhang, L.; Wu, Z. High-throughput synthesis of cross-linked poly(cyclotriphosphazene-co-bis(aminomethyl)ferrocene) microspheres and their performance as a superparamagnetic, electrochemical, fluorescent and adsorbent material. *Chem. Eng. J.* **2017**, *315*, 448–458. [CrossRef]
5. Zhou, B.; Yang, C.; Wu, F.; Deng, T.; Guo, S.; Zhu, G.; Jiang, Y.; Wang, Z. Cyclotriphosphazene-based flame-retardant polymer electrolytes for high performance sodium metal batteries. *Chem. Eng. J.* **2020**, *450*, 138385. [CrossRef]
6. Ning, K.; Zhou, L.-L.; Zhao, B. A novel aminothiazole-based cyclotriphosphazene derivate towards epoxy resins for high flame retardancy and smoke suppression. *Polym. Degrad. Stab.* **2021**, *190*, 109651. [CrossRef]
7. He, Y.-F.; Ning, K.; Zhang, C.-Y.; Shao, Z.-B.; Zhao, B. Intramolecular cooperation and biphasic flame retardant mode of action: Effectiveness of hexa(1,2,4-triazol-3-ylamine) cyclotriphosphazene in epoxy resin. *Adv. Ind. Eng. Polym. Res.* **2024**, *7*, 326–337. [CrossRef]
8. Yang, R.; Wang, B.; Han, X.; Ma, B.; Li, J. Synthesis and characterization of flame retardant rigid polyurethane foam based on a reactive flame retardant containing phosphazene and cyclophosphonate. *Polym. Degrad. Stab.* **2017**, *144*, 62–69. [CrossRef]
9. Wang, D.; Xu, X.; Qiu, Y.; Wang, J.; Meng, L. Cyclotriphosphazene based materials: Structure, functionalization and applications. *Prog. Mater. Sci.* **2024**, *142*, 101232.
10. Jamain, Z.; Khairuddean, M.; Loh, M.L.; Manaff, N.L.A.; Makmud, M.Z.H. Synthesis and characterization of hexasubstituted cyclotriphosphazene derivatives with azo linking units. *Malays. J. Chem.* **2020**, *22*, 125–140.
11. Dagdag, O.; Kim, H. Recent advances for poly(cyclotriphosphazene) functionalized graphene oxide composites: Synthesis, properties and applications. *J. Ind. Eng. Chem.* **2024**, *136*, 89–122. [CrossRef]
12. Li, Y.; Wang, B.; Sui, X.; Xie, R.; Xu, H.; Zhang, L.; Zhong, Y.; Mao, Z. Durable flame retardant and antibacterial finishing on cotton fabrics with cyclotriphosphazene/polydopamine/silver nanoparticles hybrid coatings. *Appl. Surf. Sci.* **2018**, *435*, 1337–1343. [CrossRef]
13. Allcock, H.R. The crucial role of inorganic ring chemistry in the development of new polymers. *Phosphorus Sulfur Silicon Relat. Elem.* **2004**, *179*, 661–671. [CrossRef]

14. Saini, A.; Bhedi, D.; Dhanwant, K.; Thirumoorthi, R. Multi-azobenzene moieties on rigid cyclotriphosphazene core: Synthesis, structural characterization, electrochemistry, and photoisomerization study. *J. Photochem. Photobiol. A* **2024**, *452*, 115603. [CrossRef]
15. Sönmez, E.B.; Ün, S.S.; Balcı, C.M.; Arslan, N.; Atilla, D.; Şeker, M.G.; İbişoğlu, H. New cyclotriphosphazenes with butylated oxyanisole motif; synthesis, characterization and biological properties. *Polyhedron* **2024**, *563*, 117252.
16. Zhou, F.; Xi, W.; Qian, L.; Wang, J.; Qiu, Y.; Chen, Y. Hexaphenoxy cyclotriphosphazene/boron nitride high-efficiency charring system enhancing the flame retardancy and thermal conductivity of polycarbonate. *Polym. Degrad. Stab.* **2024**, *219*, 110601. [CrossRef]
17. Doğan, S.; Tümay, S.O.; Balci, C.M.; Yeşilot, S.; Besli, S. Synthesis of New Cyclotriphosphazene Derivatives Bearing Schiff Bases and Their Thermal and Absorbance Properties. *Turk. J. Chem.* **2020**, *44*, 31–47. [CrossRef] [PubMed]
18. Waldin, N.A.; Jamain, Z. Synthesis and mechanical property of hexasubstituted cyclotriphosphazene derivatives attached to hydrazine-bridge linkage with high fire retardancy. *J. Mol. Struc.* **2023**, *1284*, 135330. [CrossRef]
19. Davarci, D.; Doganci, S. Liquid Crystal Phosphazenes. *J. Mol. Struc.* **2022**, *1269*, 133819. [CrossRef]
20. Ahmad, M.; Nawaz, T.; Hussain, I.; Chen, X.; Imran, M.; Hussain, R.; Assiri, M.A.; Ali, S.; Wu, Z. Phosphazene cyclomatrix network-based polymer: Chemistry, synthesis, and applications. *ACS Omega* **2022**, *7*, 28694–28707. [CrossRef]
21. Mathews, L.D.; Capricho, J.C.; Peerzada, M.; Salim, N.V.; Parameswaranpillai, J.; Hameed, N. Recent progress and multifunctional applications of fire-retardant epoxy resins. *Mater. Today Commun.* **2022**, *33*, 104702. [CrossRef]
22. Sulaiman, N.I.; Bakar, N.H.H.A.; Bakar, M.A. Effect of Al-Doping on Structural and Adsorption Properties of $NiFe_2O_4$ via Modified Sol–Gel Approach for CO_2 Adsorption. *Chem. Afr.* **2024**, *7*, 2139–2154. [CrossRef]
23. Palabıyık, D.; Mutlu Balcı, C.; Tümay, S.O.; Sengul, I.F.; Beşli, S. New Design of Cyclotriphosphazene Derivatives Bearing Carbazole Units: The Syntheses, Characterization, and Photophysical Properties. *Inorg. Chim. Acta* **2022**, *539*, 121022. [CrossRef]
24. Elkhalgi, H.H.M.; Khandka, S.; Singh, U.B.; Pandey, K.L.; Dabrowski, R.; Dhar, R. Dielectric and electro-optical properties of a nematic liquid crystalline material with gold nanoparticles. *Liq. Cryst.* **2018**, *45*, 1795–1801. [CrossRef]
25. Wang, J.; Liu, W.; Liu, H.; Wang, X.; Wu, D.; Zhang, S.; Shi, S.; Liu, W.; Wu, Z. Cyclotriphosphazene-based epoxy resins with excellent mechanical and flame retardant properties. *Polymer* **2022**, *261*, 125399. [CrossRef]
26. Barberá, J.; Jiménez, J.; Laguna, A.; Oriol, L.; Pérez, S.; Serrano, J.L. Cyclotriphosphazene as a dendritic core for the preparation of columnar supermolecular liquid crystals. *Chem. Mater.* **2006**, *18*, 5437–5445. [CrossRef]
27. Gioia, M.D.; Leggio, A.; Guarino, I.; Leotta, V.; Romio, E.; Liguori, A. A simple synthesis of anilines by $LiAlH_4/TiCl_4$ reduction of aromatic nitro compounds. *Tetrahedron Lett.* **2015**, *56*, 5341–5344. [CrossRef]
28. Rong, Y.; Wentian, H.; Liang, X.; Yan, S.; Jinchun, L. Synthesis, mechanical and fire behaviours of rigid polyurethane foam with a reactive flame retardant containing phosphazene and phosphate. *Polym. Degrad. Stab.* **2015**, *122*, 102–109.
29. Jamain, Z.; Khairuddean, M. Synthesis and Mesophase behaviour of benzylidene-based molecules containing two azomethine units. *J. Phys. Conf. Ser.* **2021**, *1882*, 012120. [CrossRef]
30. Fang, Z.; Liu, Y.; Zhang, Y.; Cao, Z. Phosphorus-Containing Schiff Base Derivative Expanded Flame Retardant and Its Preparation. CN Patent No. CN102732041A, 29 May 2012.
31. Jamain, Z.; Khairuddean, M.; Guan-Seng, T. Liquid-Crystal and Fire-Retardant Properties of New Hexasubstituted Cyclotriphosphazene Compounds with Two Schiff Base Linking Units. *Molecules* **2020**, *25*, 2122. [CrossRef]
32. Rajkumar, P.; Selvaraj, S.; Anthoniammal, P.; Ram Kumar, A.; Kasthuri, K.; Kumaresan, S. Structural (monomer and dimer), spectroscopic (FT-IR, FT-Raman, UV–Vis and NMR) and solvent effect (polar and nonpolar) studies of 2-methoxy-4-vinyl phenol. *Chem. Phys. Impact.* **2023**, *7*, 100257. [CrossRef]
33. Kara, Y.S.; Diran, D. Synthesis of novel 1,2,4-oxadiazine derivatives and the substituent effect study on ^{13}C NMR spectra. *J. Mol. Struct.* **2024**, *1310*, 138309. [CrossRef]
34. Kara, Y.S.; Yıldız, B. Synthesis and substituent effect study on ^{13}C NMR chemical shifts of 4-(substitue-phenyl)-6-methyl-3-phenyl-4H-1,2,4-oxadiazin-5(6H)-one. *J. Mol. Struct.* **2022**, *1250*, 131787. [CrossRef]
35. Kupka, T.; Dziuk, B.; Ejsmont, K.; Makieieva, N.; Fizer, L.; Monka, N.; Konechna, R.; Stadnytska, N.; Vasyliuk, S.; Lubenets, V. Impact of crystal and molecular structure of three novel thiosulfonate crystals on their vibrational and NMR parameters. *J. Mol. Struct.* **2024**, *1313*, 138642. [CrossRef]
36. Jamain, Z.; Khairuddean, M.; Kamaruddin, K.; Rui, Y. Synthesis, structural elucidation and mesophase behavior of hexasubstituted cyclotriphosphazene molecules with amide linking unit. *Malays. J. Chem.* **2021**, *23*, 213–225.

Disclaimer/Publisher's Note: The statements, opinions and data contained in all publications are solely those of the individual author(s) and contributor(s) and not of MDPI and/or the editor(s). MDPI and/or the editor(s) disclaim responsibility for any injury to people or property resulting from any ideas, methods, instructions or products referred to in the content.